RANSAC-Based Planar Point Cloud Segmentation Enhanced by Normal Vector and Maximum Principal Curvature Clustering

Yibo Ling[1], Yuli Wang[1], Ting On Chan[1] *

[1] School of Geography and Planning, Sun Yat-sen University, 510275 Guangzhou, China - (lingyb3, wangyli56)@mail2.sysu.edu.cn, chantingon@mail.sysu.edu.cn

Keywords: Point Cloud, Plane Segmentation, Region Growing, Maximum Principal Curvature, RANSAC.

Abstract:

Planar feature segmentation is an essential task for 3D point cloud processing, finding many applications in various fields such as robotics and computer vision. The Random Sample Consensus (RANSAC) is one of the most common algorithms for the segmentation, but its performance, as given by the original form, is usually limited due to the use of a single threshold and interruption of similar planar features presented close to each other. To address these issues, we present a novel point cloud processing workflow which aims at developing an initial segmentation stage before the basic RANSAC is performed. Initially, normal vectors and maximum principal curvatures for each point of a given point cloud are analyzed and integrated. Subsequently, a subset of normal vectors and curvature is utilized to cluster planes with similar geometry based on the region growing algorithm, serving as a coarse but fast segmentation process. The segmentation is therefore refined with the RANSAC algorithm which can be now performed with higher accuracy and speed due to the reduced interference. After the RANSAC process is applied, resultant planar point clouds are built from the sparse ones via a point aggregation process based on geometric constraints. Four datasets (three real and one simulated) were used to verify the method. Compared to the classic segmentation method, our method achieves higher accuracy, with an RMSE from fitting equal to 0.0521 m, along with a higher recall of 93.31% and a higher F1-score of 95.38%.

1. Introduction

Light Detection and Ranging (LiDAR, renowned for its ability to promptly generate detailed three-dimensional (3D) spatial data. With the advancement of hight-precision LiDAR sensors, an increasing array of fields are incorporating this technology, such as autonomous vehicles (Li and Ibanez-Guzman, 2020 , Zhao et al., 2020), cultural heritage management (Chan et al., 2011 , Rodríguez-Gonzálvez et al., 2017 , Chan et al., 2021, Teppati Losè et al., 2022), mobile robotics (Weiss and Biber, 2011 , Yang et al., 2022), and smart cities (Garnett and Adams, 2018 , Ortega et al., 2021). Three-dimensional point clouds, as a data type for recording LiDAR measurements, require extensive post-processing in which the plane segmentation is one of most significant processing operations.

Plane segmentation algorithms can be broadly categorized into two types: parameter-based methods and clustering-based methods (Wu et al., 2019). For parameter-based methods, the RANSAC algorithm (Fischler and Bolles, 1981) is one of the most frequently-used due to its robustness. It operates by iteratively selecting random points to construct initial planes, then extracting the best-fitting plane by comparing the number of points falling on each plane. Kurban et al. (2015) utilized RANSAC algorithm to segment point cloud obtained from Kinect sensor. Qian and Ye (2014) combine the Normalized Cross-Correlation technique with the RANSAC algorithm to swiftly and accurately identify planar surfaces in complex 3D scenes. Li and Shan (2022) utilizes the RANSAC algorithm to identify and extract multiple primitive shapes or structures that collectively represent a building. While this approach can reduce the influence of outliers, it often requires considerable time to identify the correct plane and can sometimes segment numerous inaccurate planes in complex scenes, such as those involving stairways point cloud (Awwad et al., 2010). Nonetheless, the clustering-based methods group points that are close in both normal vectors and spatial positions. For example, Xu et al. (2019) employed an improved density clustering algorithm to group points together, facilitating the identification and fitting of planes in the point cloud data.

Sağlam et al. (2020) segmented the point cloud data into patches using K-means clustering and then refining these non-planar patches into plane segments. These methods typically cluster points based on either spatial proximity or normal vectors at a time, often requiring a secondary segmentation step. Region growing algorithm (Gorte, 2002 , Tóvári and Pfeifer, 2005 , Nurunnabi et al., 2012) is another clustering-based plane segmentation method that can simultaneously consider both spatial and normal vector information. However, it currently faces challenges related to slow computational speed and the selection of an appropriate seed point strategy (Wu et al., 2019).

In order to accelerate the speed of the point-based region growing and to enhance the precision of the original RANSAC algorithm for plane segmentation in complex scenes, we present a comprehensive workflow that it begins with an initial segmentation operation on downsampled point clouds, employing a seed point selection strategy based on finding the minimum value of the maximum principal curvature. Following this initial segmentation, the algorithm uses the obtained information to perform the secondary segmentation on the original point cloud data with RANSAC algorithm and distance and normal vector constrained clustering.

2. Method

Firstly, local regions' normal vectors and maximal principal curvature are estimated by constructing a K-d tree structure (Friedman et al., 1977) to search for the adjacent points of each point. The normal vectors are estimated by calculating the three principal components of the local point cloud and taking the

* Corresponding author

direction of the third principal component as its estimate. Subsequently, a downsampling operation is employed to accelerate the coarse segmentation of the subsequent region growing algorithm. Since a portion of the planar points has already been clustered, the RANSAC algorithm can more rapidly identify the correct plane through random point selection and obtain the corresponding plane parameters. Finally, based on the obtained plane parameters, the distance from the original point cloud before downsampling to each plane is calculated. The final segmentation of the planar point cloud is obtained through constraints based on distance and normal vectors. The described workflow is shown in Figure 1.

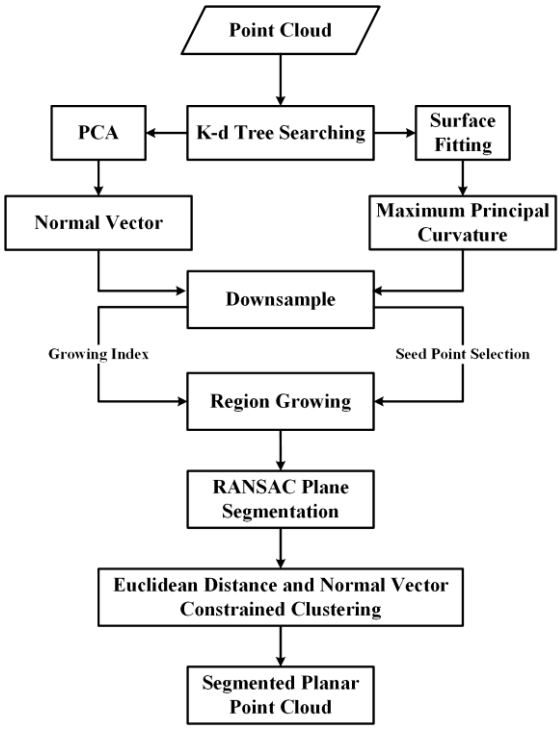

Figure 1. Workflow of our method.

2.1 Normal Vector and Maximum Principal Curvature

The local adjacent points obtained by K-d tree searching algorithm is fitted to the surface to estimate the normal vector and maximum principal curvature. Principal Component Analysis (PCA) is employed to calculate the three principal components for each local region of the point cloud (Jolliffe, 2002). Based on the planar characteristics, the eigenvector corresponding to the smallest eigenvalue represents the direction with the least information, which is perpendicular to the local plane and can be used as an estimation for the normal vector (Hoppe et al., 1992).

The normal curvature of a point is the degree of curvature of the intersection curve between the surface and a plane, which passes through that point and is perpendicular to the tangent plane. The planes that meet the above conditions are countless, and the principal curvatures are the two curvatures among them that represent the maximum and minimum degrees of curvature (Figure 2). The maximum principal curvature (Gray, 1997) is incorporated into our method.

After performing a least squares quadratic surface fitting (Eq. 1) to the adjacent point cloud, Gaussian curvature and mean curvature (Gray, 1997) can be obtained using the Eq. (2-3), and subsequently solving the Eq. (4-5) yields the maximum principal curvature.

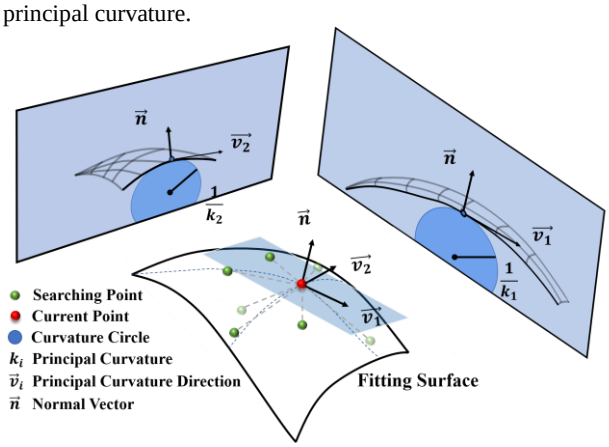

Figure 2. Principal curvature viewed from two different angles.

$$F(x,y,z) = z - \left(ax^2 + bxy + cy^2\right) = 0 \tag{1}$$

$$M = \frac{\left(1+z_x^2\right)z_{yy} - 2z_x z_y z_{xy} + \left(1+z_y^2\right)z_{xx}}{2\left(1+z_x^2+z_y^2\right)^{\frac{3}{2}}} \tag{2}$$

$$G = \frac{z_{xy}^2 - z_{xx}\cdot z_{yy}}{\left(1+z_x^2+z_y^2\right)^2} \tag{3}$$

$$G = k_1 k_2 \tag{4}$$

$$M = \frac{k_1 + k_2}{2} \tag{5}$$

where G, M are Gaussian curvature and mean curvature respectively, k_i denotes principal curvature.

2.2 Region Growing based on Geometric Parameters

The region growing algorithm can be used to aggregate points with similar normal vectors and proximity in distance. This algorithm fundamentally begins from a set of seed points and progressively incorporates adjacent points into the region of these seed points, guided by specific criteria. The process continues until certain predetermined stopping conditions are met. The key to the region growing algorithm’s effectiveness lies in the strategies employed for selecting seed points and defining criteria for the inclusion of adjacent points.

For planar point clouds, the degree of curvature is approximately zero, and the normal vectors are similar throughout the same plane. Consequently, curvature can be adopted as a criterion for selecting seed points, and the angle between normal vectors (Θ) can serve as a condition for growth. In this paper, the point with the smallest maximum principal curvature is selected as the seed point and the angle between the normal vectors serves as the growth condition. The complete workflow can be seen in Figure 3.

This contribution has been peer-reviewed. The double-blind peer-review was conducted on the basis of the full paper.
https://doi.org/10.5194/isprs-annals-X-1-2024-145-2024 | © Author(s) 2024. CC BY 4.0 License.

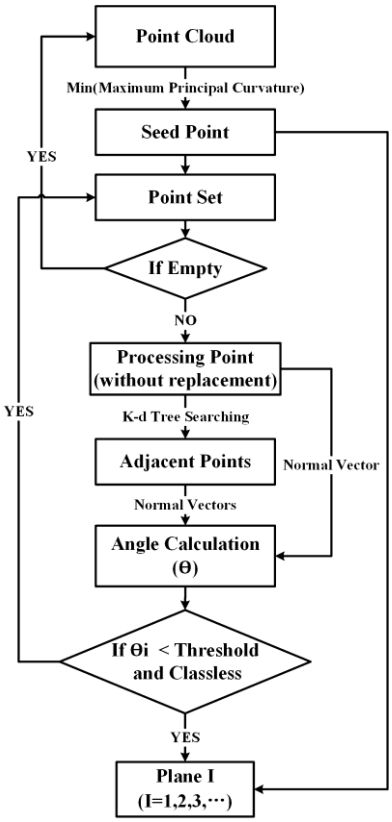

Figure 3. Workflow of region growing for geometric parameters.

2.3 Segmentation Result Evaluation

The accuracy of the final segmented planar will be assessed using the root mean square error (RMSE) of the parameters fitted through least squares method (Eberly, 2000), and the average precision, recall, F1-score of the segmented point clouds for multiple planes. This evaluation will be conducted on simulated stairway data. The equation as follow:

$$RMSE_{average} = \frac{1}{N}\sum_{i=1}^{N}\sqrt{\frac{1}{4}\sum_{j=1}^{4}(P_{ij} - P_{ij}')^2} \quad (6)$$

$$Precision_{average} = \frac{1}{N}\sum_{i}^{N}\frac{TP_i}{TP_i + FP_i} \quad (7)$$

$$Recall_{average} = \frac{1}{N}\sum_{i}^{N}\frac{TP_i}{TP_i + FN_i} \quad (8)$$

$$F1-score_{average} == \frac{1}{N}\sum_{i}^{N}\frac{2\times Precision_i \times Recall_i}{Precision_i + Recall_i} \quad (9)$$

where N is the number of planes, P_{ij} and P_{ij}' respectively represent the fitted and true values of the j-th parameter of the i-th plane, TP_i represents the number of points correctly classified as belonging to plane i, FN_i represents the number of points incorrectly classified as not belonging to plane i, FP_i represents the number of points incorrectly classified as belonging to class i.

3. Experiments

We applied our method to point clouds from four different scenes, and compared it with classic RANSAC plane segmentation and region growing methods in terms of visual effects and computational speed. quantitative accuracy. Additionally, the segmentation results of each method were quantitatively evaluated using a simulated stairway point cloud data.

The experimental data for this study consists of point cloud data from four different scenes: (1) A room point cloud at a university, acquired by a Trimble SX 10 scanner, consisting of 538099 points (Figure 4a). (2) A simulated straight stairway point cloud, composed by stitching together seven rectangular cuboid point clouds with 0.01 m Gaussian noise, consisting of 167556 points (Figure 4b). (3) A spiral stairway point cloud at a university, obtained by a Trimble SX 10 scanner, consisting of 526706 points (Figure 4c). (4) An electric tower body point cloud, collected by a Faro Focus^{3D} scanner, consisting of 569667 points (Figure 4d).

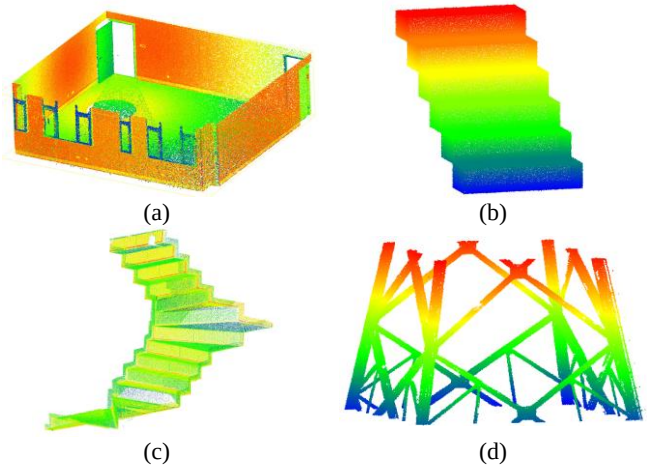

Figure 4. (a) Scene 1: a room at the university (real point cloud). (b) Scene 2: a straight stairway (simulated point cloud). (c) Scene 3: a spiral stairway at a university (real point cloud). (d) Scene 4: a electric tower body (real point cloud).

4. Results

4.1 Preliminary Plane Segmentation

In the scenes with planes, the distribution of normal vectors presents a clustered state (Figure 5). However, due to the influence of point cloud noise and errors in the normal vector estimation method, especially significant at the edges of planes, the planar points clustered by region growing often has omissions (Figure 6).

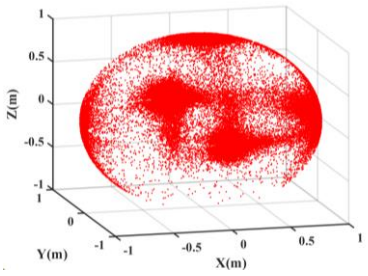

Figure 5. Normal sphere (such as Scene 1).

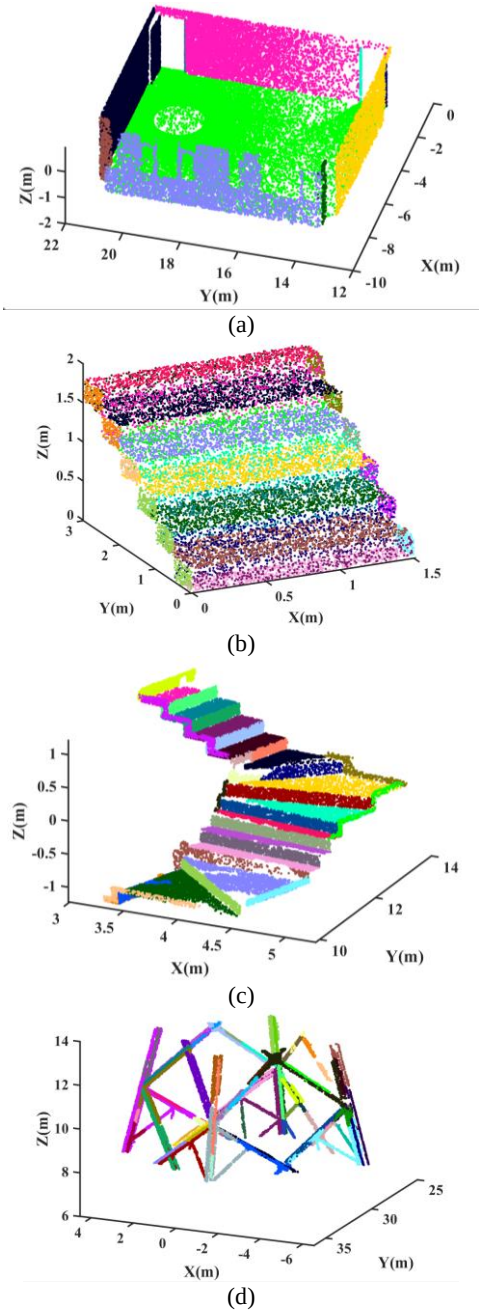

Figure 6. Preliminary Plane Segmentation Results of Region Growing (Different colours represent different planes). (a) Scene 1. (b) Scene 2. (c) Scene 3. (d) Scene 4.

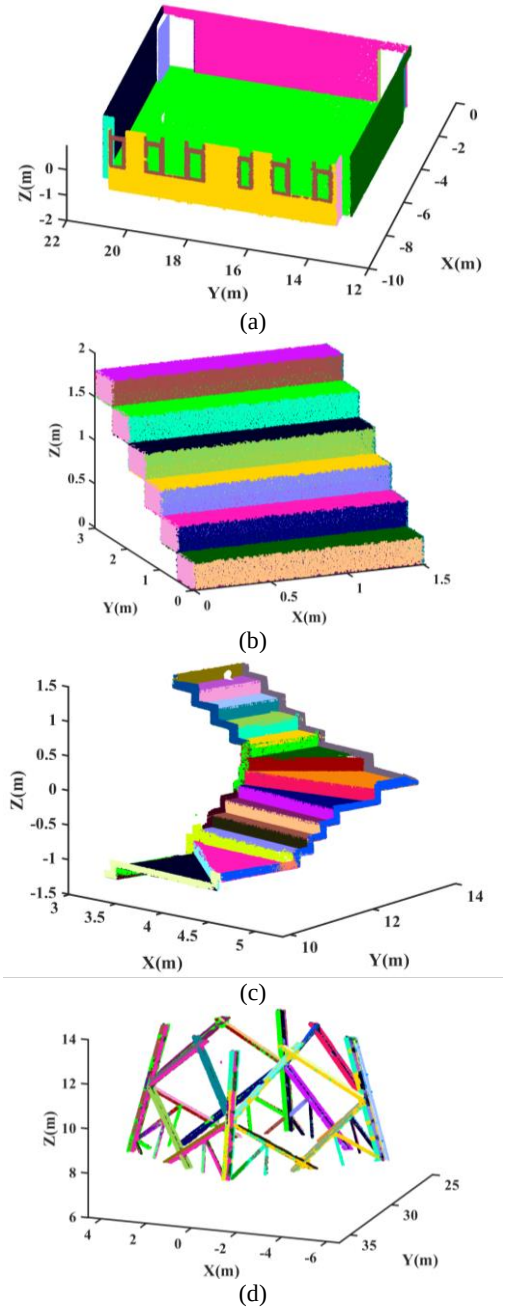

Figure 7. Final segmented point cloud (Different colours represent different planes). (a) Scene 1. (b) Scene 2, (c) Scene 3. (d) Scene 4.

4.2 Final Plane Segmentation

During the RANSAC algorithm process, iterative searches are conducted to find planar points, and the preliminarily segmented planar points can enable it to fit rapidly. Finally, based on the information of the fitted planes, coupled with constraints on the point-to-plane distance and normal vectors, complete planar points are segmented from the original dense point cloud. Figure 7 are the final segmented results of our method.

4.3 Comparison

The classic RANSAC method and region growing method were used to segment the point clouds of these four scenes, and the results are shown in Figure 8. Additionally, the operating speeds of different methods were compared, and the results are presented in Table 1.

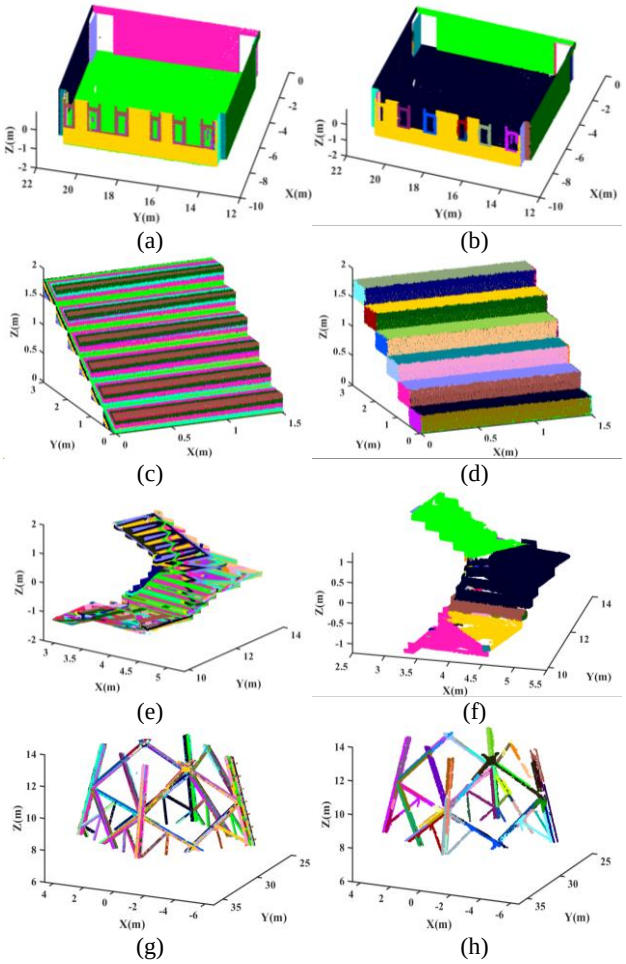

Figure 8. The results of classic RANSAC. (a) Scene 1. (c) Scene 2. (e) Scene 3. (g) Scene 4. The results of classic region growing. (b) Scene 1. (d) Scene 2. (f) Scene 3. (h) Scene 4.

It is evident that the RANSAC method tends to segment numerous inaccurate planes, such as the window frame in Scene 1 and the inclined planes in Scene 2 and Scene 3. For the region-growing algorithm, the segmentation result for Scene 2 is quite good, but there were some errors in Scene 1 and 3. For instance, in Scene 1, the mutually perpendicular left plane and bottom plane were segmented as a single plane, while in Scene 3, multiple steps were segmented as one plane, which are mainly due to the inaccurate estimation of normal vectors. In the case of the most complex Scene 4, although all three methods exhibit some confusions, our method demonstrates a slightly lower error rate in terms of visual effectiveness.

Table 1. Operating Speed of Different Methods.

	Scene 1	Scene 2	Scene 3	Scene 4
No. of points	538099	167556	526706	569667
No. of planes	9	16	30	>30
T_{RANSAC} (s)	2.04	13.79	248.27	298.05
T_{RG} (s)	671.72	418.57	9252.51	30201.46
T_{Our} (s)	46.95	6.61	112.08	107.28

In comparison to these two methods, our approach exhibits superior segmentation results visually. In terms of speed, the region growing algorithm is the slowest because it requires iterative searching of adjacent points for growth. Since our method also employs the region growing algorithm, its operating speed is not as fast as the RANSAC method when dealing with a large number of point clouds. Additionally, an increase in the number of point clouds will lead to longer times for calculating curvature and normal vectors. However, the use of a K-d tree can accelerate this process to a certain extent. Due to the fact that the speed of RANSAC also depends on the number of planes in the scenes, our algorithm achieves a reverse exceedance in speed when processing scenes with multiple planes such as Scene 2, 3 and 4, where it is faster by 7.18 s, 136.19 s and 190.77 s, respectively. Compared to the region growing algorithm, the speed of our method is significantly faster, being respectively 624.77 s, 411.96 s, 9140.43 s and 30094.18s quicker in Scene 1, 2, 3 and 4.

Due to the generation of numerous inaccurate segmented planes by RANSAC in the simulated stair point cloud, quantitative accuracy evaluation was conducted exclusively for our method and the region growing algorithm. The results of accuracy evaluation are shown in Table 2. Our method demonstrated higher accuracy, achieving an average RMSE of 0.0521 m, which is superior to the region growing algorithm at 0.116 m. Although our method is approximately 1% lower in precision compared to region growing, our recall and F1-score are higher by 3.86% and 1.68%, respectively. This indicates that our method exhibits fewer cases of both error and missed segmentations, demonstrating its robustness.

Table 2. RMSE of plane parameters for different methods.

	RG	Ours
Average RMSE (m)	0.1681	**0.0521**
Precision (%)	**98.52**	97.54
Recall (%)	89.45	**93.31**
F1-score (%)	93.76	**95.38**

At the end of this paper, we replaced the RANSAC algorithm with the least squares method to fit the plane on the preliminarily segmented point cloud, in order to validate the necessity and superiority of the RANSAC method in our method. Due to the sensitivity of the least squares method to noise, there exists a problem of parameter bias in the fitting process, leading to errors in plane segmentation, as illustrated in the first stair shown in Figure 9b.

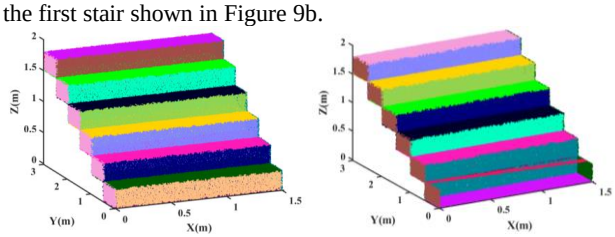

Figure 9. (a) Region-growing-RANSAC segmentation result for Scene 2. (b) Region-growing-least-squares segmentation result for Scene 2.

5. Conclusion

This paper proposes an algorithm that clusters points with similar normal vectors and spatial proximity in a downsampled point cloud to enhance the subsequent RANSAC-based plane segmentation process. The algorithm is both fast and accurate, addressing the efficiency issues of region-growing algorithms and the problem of inaccurate segmented plane generation in classic RANSAC algorithms. Furthermore, the algorithm offers a strategy for selecting seed points for the region-growing

algorithm based on the minimal value of the maximum principal curvature. Through comparative experiments applying three different methods to four different scenes, our approach demonstrates the best visual effects and superior computational efficiency. Additionally, it exhibits the highest accuracy in terms of RMSE, recall, and F1-score, achieving 0.0521m, 93.31%, and 95.38%, respectively. The results indicate the superiority of our workflow in terms of execution speed and accuracy. Our study integrates normal vector clustering constraints into plane segmentation algorithms, leveraging the strengths of both region-growing and RANSAC techniques. This fusion aims to enhance the robustness of plane segmentation methods, providing a directional reference for research in this field.

References

Awwad T.M., Zhu Q., Du Z., Zhang Y., 2010. An improved segmentation approach for planar surfaces from unstructured 3D point clouds. *The Photogrammetric Record*, 25, 5-23.

Chan, T.O., Sun, Y., Yu J., Zeng, J. and Liu, L., 2021. Symmetry etection and Analysis of Chinese Paifang Using 3D Point Clouds. *Symmetry*, 13, 2011.

Chan, T.O., Xiao H., Liu, L., Sun, Y., Chen, T., Lang, W., Li, M. H., 2021. A Post-Scan Point Cloud Colorization Method for Cultural Heritage Documentation, *ISPRS International Journal of Geo-Information*, 2021 (10),737.

Eberly D., 2000. Least squares fitting of data. *Chapel Hill, NC: Magic Software*, 2000: 1-10.

Fischler M.A., Bolles R.C., 1981. Random sample consensus: a paradigm for model fitting with applications to image analysis and automated cartography. *Communications of the ACM*, 24, 381-395.

Friedman J.H., Bentley J.L., Finkel R.A., 1977. An algorithm for finding best matches in logarithmic expected time. *ACM Transactions on Mathematical Software (TOMS)*, 3, 209-226.

Garnett R., Adams M.D., 2018. LIDAR—A technology to assist with smart cities and climate change resilience: A case study in an urban metropolis. *ISPRS International Journal of Geo-Information*, 7, 161.

Gorte B., 2002. Segmentation of TIN-structured surface models. *International Archives of Photogrammetry Remote Sensing and Spatial Information Sciences*, 34, 465-469.

Gray A., 1997. The gaussian and mean curvatures. *Modern differential geometry of curves and surfaces with mathematica*, 2, 373-380.

Gray, A., 1997. Normal Curvature. *Modern Differential Geometry of Curves and Surfaces with Mathematica*, 2, 363-367.

Hoppe H., Derose T., Duchamp T., Mcdonald J., Stuetzle W., 1992. Surface reconstruction from unorganized points. *Proceedings of the 19th annual conference on computer graphics and interactive techniques*, 71-78.

Jolliffe I.T., 2002: *Principal component analysis for special types of data*. Springer.

Kurban, R., Skuka, F., Bozpolat, H., 2015. Plane segmentation of kinect point clouds using RANSAC. *7th International Conference on Information Technology, ICIT, Amman, Jordan*, 545-551.

Li Y., Ibanez-Guzman J., 2020. Lidar for autonomous driving: The principles, challenges, and trends for automotive lidar and perception systems. *IEEE Signal Processing Magazine*, 37, 50-61.

Li, Z., Shan, J., 2022. RANSAC-based multi primitive building reconstruction from 3D point clouds. *ISPRS Journal of Photogrammetry and Remote Sensing*, 185, 247-260.

Nurunnabi A., Belton D., West G., 2012. Robust Segmentation in Laser Scanning 3D Point Cloud Data. *2012 International Conference on Digital Image Computing Techniques and Applications (DICTA)*, 1-8.

Ortega S., Santana J.M., Wendel J., Trujillo A., Murshed S.M., 2021. Generating 3D city models from open LiDAR point clouds: Advancing towards smart city applications. *Open Source Geospatial Science for Urban Studies: The Value of Open Geospatial Data*, 97-116.

Qian, X., Ye, C., 2014. NCC-RANSAC: A fast plane extraction method for 3-D range data segmentation. *IEEE transactions on cybernetics*, *44*(12), 2771-2783.

Rodríguez-Gonzálvez P., Jimenez Fernandez-Palacios B., Muñoz-Nieto Á. L., Arias-Sanchez P., Gonzalez-Aguilera D., 2017. Mobile LiDAR system: New possibilities for the documentation and dissemination of large cultural heritage sites. *Remote Sensing*, 9, 189.

Sağlam, A., Makineci, H. B., Baykan, Ö. K., Baykan, N. A., 2020. Clustering-based plane refitting of non-planar patches for voxel-based 3D point cloud segmentation using k-means clustering. *Traitement du Signal*.

Teppati Losè L., Spreafico A., Chiabrando F., Giulio Tonolo F., 2022. Apple LiDAR Sensor for 3D Surveying: Tests and Results in the Cultural Heritage Domain. *Remote Sensing*, 14, 4157.

Tóvári D., Pfeifer N., 2005. Segmentation based robust interpolation-a new approach to laser data filtering. *International Archives of Photogrammetry, Remote Sensing and Spatial Information Sciences*, 36, 79-84.

Weiss U., Biber P., 2011. Plant detection and mapping for agricultural robots using a 3D LIDAR sensor. *Robotics and autonomous systems*, 59, 265-273.

Wu H., Zhang X., Shi W., Song S., Cardenas-Tristan A., Li K., 2019. An accurate and robust region-growing algorithm for plane segmentation of TLS point clouds using a multiscale tensor voting method. *IEEE Journal of Selected Topics in Applied Earth Observations and Remote Sensing*, 12, 4160-4168.

Xu, X., Luo, M., Tan, Z., Zhang, M., Yang, H., 2019. Plane segmentation and fitting method of point clouds based on

improved density clustering algorithm for laser radar. *Infrared Physics & Technology*, 96, 133-140.

Yang T., Li Y., Zhao C., Yao D., Chen G., Sun L., Krajnik T., Yan Z., 2022. 3D ToF LiDAR in mobile robotics: A review. *arXiv preprint arXiv:2202.11025*.

Zhao X., Sun P., Xu Z., Min H., Yu H., 2020. Fusion of 3D LIDAR and camera data for object detection in autonomous vehicle applications. *IEEE Sensors Journal*, 20, 4901-4913.